HEATING AND COOLING CAPACITY OF PHASE CHANGE MATERIAL COUPLED WITH SCREEN MESH WICK HEAT PIPE FOR THERMAL ENERGY STORAGE APPLICATIONS

Rajendran Ramesh PALAPPAN[1*], Avadaiappa Pillai PASUPATHY[2],

Lazarus Godson ASIRVATHAM[3], Trijo THARAYIL[4], Somchai WONGWISES[5, 6*]

[1]Research scholar, Anna University, Chennai, Tamil Nadu, India, 600025

[2]SECAB Institute of Engineering & Technology, Jala Nagar, Vijayapura, Karnataka, 586109

[3]Department of Mechanical & Aerospace Engineering, Karunya Institute of Technology and Sciences, Coimbatore, India, 641114

[4]Department of Mechanical Engineering, Sree Buddha College of Engineering, Pattoor, Alappuzha, India, 690529

[5]Fluid Mechanics, Thermal Engineering and Multiphase Flow Research Lab (FUTURE), Department of Mechanical Engineering, Faculty of Engineering, King Mongkut's University of Technology Thonburi,126 Bangmod, Tongkru, Bangkok 10140, Thailand.

[6]The Academy of Science, The Royal Society of Thailand, Sanam Suea Pa, Dusit, Bangkok 10300, Thailand

[*] Corresponding author; E-mail: rrameshpalappan@gmail.com, somchai.won@kmutt.ac.th

The thermal performance of a phase change material-heat pipe system is experimentally analysed using acetone as heat pipe fluid in a heat load range of 10-50W at different flow rates of the condenser coolant. The evaporator of the heat pipe is enclosed in a chamber which filled with a phase change material or water. Heat inputs are applied at the evaporator of the heat pipe through the phase change material or water. In this study, the heat retention as well as cooling time of the phase change material/water are estimated at different heat loads and flow rates of condenser coolant. Similarly, the thermal resistance, evaporator and condenser heat transfer coefficients are also estimated at different heat loads. It is observed that the phase change material takes more time during heating and cooling cycles to reach the steady state temperatures and the temperature values reached during heating are also higher for phase change material compared to water. The use of phase change material enhances the thermal storage capacity and shows a maximum enhancement of 200% in heat retention time compared to water at 50W. Moreover, a maximum enhancement of 63.6% is observed in the steady state temperature of the phase change material compared to water. Similarly thermal resistance, evaporator wall temperature and heat transfer coefficients of the heat pipe also vary for

phase change material and water. The experimental results indicate that phase change material or water can be used in this combined system depending upon requirement of thermal storage or electronics cooling.
Keywords: *Heat pipe, PCM, Thermal energy storage, Latent heat, Electronic cooling*

1. Introduction

Thermal energy storage has gained attention of researchers in the recent years as the stored thermal energy can be used in various applications. These applications include heat pipe, heat pumps, solar thermal applications, space craft thermal control and transient electronic cooling applications such as personal computing, cell phones and digital video cameras [1-3]. Phase change materials (PCMs) are considered as one of the effective methods for the thermal energy storage because they store the energy as latent heat [4]. A few researchers have also suggested PCMs for cooling of electronic devices as described below.

Tan and Tso [5] used n-eicosane as a PCM inside electronic devices and found that a larger amount of PCM could improve the stability and safety of electronic devices. Arshad et al. [6] reported that the use of PCM helped to keep the electronic devices in their safe temperature limits. Ali and Arshad [7] also recommended the use of PCM in heat sink for cooling of electronic devices. Arshad et al. [8] studied the effect of paraffin wax, which is a PCM material, on the thermal management of electronic devices by incorporating PCM at the heat sink. Ashraf et al. [9] compared the thermal performance of various PCMs using different heat sink designs to meet the electronic cooling requirements. It was reported that the performance of PCM at lower and higher power levels are different and it was due to change in properties of the PCM at various temperatures. Yoo and Joshi [10] manufactured grooves inside the plate fin and pin fin, filled these with PCM to promote heat handling capability. Zheng and Wirtz [11, 12] exploited the high storage density characteristic of PCM to reduce fan power consumption of electronic devices up to 12.4%. Similarly, other researchers have also investigated the PCM characteristics with the aim of improving the thermal energy storage and electronic cooling [13-14].

Heat pipes are also used for cooling of various electronic devices to maintain device temperature in safe limits for the reliable operation. Heat pipes offer large heat transfer rates because they exploit the benefits of boiling and condensation. Many researchers have recommended the use of heat pipes for electronic cooling applications as described below. Asirvatham et al. [15] experimentally studied the heat transfer performance of a screen mesh wick heat pipe and reported the suitability of heat pipes for electronic cooling requirements. Kumaresan et al. [16] compared the performance of sintered and mesh wick heat pipes at various heat loads and also suggested both heat pipes to cool electronic devices. Similarly, many other researchers have suggested the combined use of heat pipe and nanofluid to get maximum heat transfer [17-30].

A few researchers have coupled both PCM and heat pipe for various thermal storage and cooling applications as described below. Ladekar et al. [31] analysed the thermal performance of PCM-Heat pipe coupled system at various flow rates of the heat transfer fluid using paraffin wax as the PCM. It was observed that the coupled system has more efficiency in terms of heat absorption and rejection. Wu et al. [32] used a PCM-heat pipe coupled system for the battery thermal management. The experimental study showed that the battery can be maintained below 50^{o}C by utilizing the thermal

storage and cooling capabilities of PCM and heat pipe respectively. Tiari et al. [33] used Rubitherm RT55 as PCM for thermal energy storage in a system having heat pipe network and investigated the effect of temperature and flow rates of the heat transfer fluid. It was observed that both flow rate and temperature were important as far as charging and discharging processes were concerned. Motahar and Khodabandeh [34] conducted an experimental study to analyze the melting and solidification processes which occur in PCM-heat pipe coupled system. The experimental results showed the improvement in heat transfer from and to the PCM with the PCM-heat pipe coupled system. Similarly a few researchers have highlighted the properties of PCM in their research which also recommends the use of PCM-heat pipe systems [35-39].

Hence, it can be concluded that the benefits of PCM and heat pipe can be combined when PCM-heat pipe coupled systems are used. To the best of authors' knowledge, only a very few research has been conducted using OM32 as phase change material in a cylindrical screen mesh wick heat pipe-PCM coupled system. Similarly, the heat retention and releasing time of OM32 by using it as the heating source at the evaporator section of the cylindrical screen mesh wick heat pipe has not been studied so far. Hence, in the present study, the heating and cooling capacities of the PCM (OM32) are experimentally studied with different heat load (10 to 50 W) conditions and flow rates of coolant at condenser using a PCM-heat pipe coupled system in vertical orientation. The heat pipe used is a copper screen mesh wick heat pipe. The heat is supplied at the evaporator of the heat pipe through a container filled with PCM/water. The heating and cooling cycles for PCM and water are analysed along with heat pipe thermal performance.

2. Experimental investigations

2.1. Experimental setup and procedure

Fig. 1 (a) shows the experimental setup, which includes heat pipe, thermal energy storage tank, chilling unit, pump, rotameter, heater, power supply, computer, and a data logger. The heat pipe shown in Fig. 1 (a) is a cylindrical heat pipe made of copper having 11.5mm and 12.7mm inner and outer diameters respectively and 300mm length with a wall thickness of 0.6mm. The lengths of evaporator, adiabatic and condenser sections of the heat pipes are 100mm, 50mm and 150 mm respectively. Three layers of copper wick with a wire diameter of 0.105mm and mesh size of 100/inch is wrapped inside the heat pipe as shown in Fig. 1 (b) and (c). A filling ratio of 30% of the total volume of the heat pipe is charged into the heat pipe at a low a pressure to completely saturate the wick. The condenser section of the heat pipe is a water cooled heat exchanger made up of acrylic material. Cooling water at a various flow rate of 6, 7.5, 8.5 and 10 LPH is circulated through the condenser in order to absorb the heat from the heat pipe at the condenser section. Table 1 shows the full specification of the PCM-heat pipe system.

A chilling unit is used to maintain the inlet temperature of the circulating cooling water at 20^0C for all the tests. The temperatures of the cooling water circulating through the condenser section are recorded using two T-type thermocouples fixed at inlet and outlet of the condenser. The accuracy of the thermocouples is $\pm 0.5^o$C. A total of nine T-type thermocouples are fixed at various locations along the test section as shown in Fig. 1 (a). The heat input to the heat pipe is applied using a digital watt meter (with an uncertainty of ±0.5W) connected to an electric heater which is at the bottom of thermal energy storage tank on the evaporator section. A 220V A.C supply is used to energize the heater for heating the PCM and water. The heat pipe receives heat from the fluid filled in the thermal storage

tank. The evaporator with thermal energy storage tank and adiabatic sections of the heat pipe are completely insulated using glass wool insulation in order to minimize the heat loss to the ambient. The temperature readings of the test section are recorded by the data logger (Agilent 34972 A). The readings are taken at regular intervals of time (30s) until the steady state is reached. The entire data acquisition system is connected to a computer. The stored data is used for the data analysis.

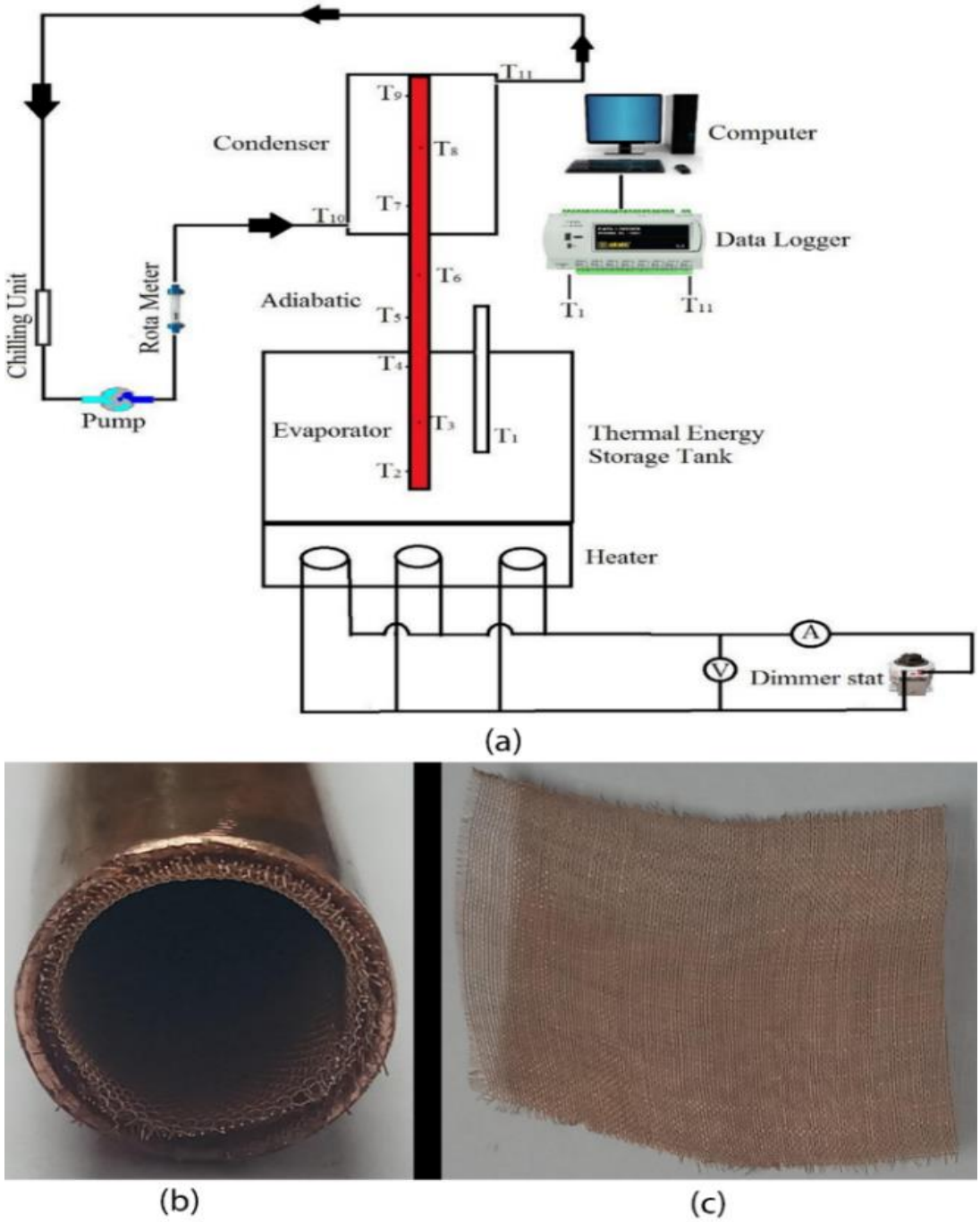

Fig. 1(a) Experimental setup, (b) three layers of copper wick and (c) copper wire mesh

Table 1. Specification of the PCM heat pipe system

Specification	Dimension/Material
Overall length	300mm
Material of pipe	Copper
Diameter of HP (outer)	12.7mm
Diameter of HP (inner)	11.5mm
Wall thickness of HP	0.6mm
Length of evaporator region	100mm
Length of adiabatic region	50mm
Length of condenser region	150mm
Wick type	Screen mesh wick
Wick material	Copper
Wick porosity	63%
Wick thickness	0.25mm
Number of wick layers	3
Diameter of cylindrical condenser	35mm
Length of condenser	150mm
Thickness of condenser	3mm
Material of condenser	Acrylic
Diameter of thermal storage tank	50mm
Height of thermal storage tank	120mm
Working fluid of heat pipe	Acetone
Working fluid loading	6 ml

2.2. Data reduction

The average evaporator and condenser surface temperatures (T_{we} and T_{wc}) are calculated using Eq. (1) and Eq. (2).

$$T_{we} = \frac{T_2 + T_4}{2} \tag{1}$$

$$T_{wC} = \frac{T_7 + T_9}{2} \tag{2}$$

The ratio of (T_{we}-T_{wc}) to the applied heat input (Q) is known as thermal resistance of heat pipe (R_t) and it is calculated using the Eq. (3).

$$R_t = \frac{T_{we} - T_{wc}}{Q} \tag{3}$$

The ratio of applied heat input (Q) to the product of evaporator surface area (A_e) and the temperature difference between surface (T_{we}) and vapour (T_{ve}) in the evaporator region is known as evaporator heat transfer coefficient (h_e) and the same is calculated using the Eq. (4).

$$h_e = \frac{Q}{A_e[T_{we} - T_{ve}]} \tag{4}$$

The ratio of condenser heat output (Q_c) to the product of condenser surface area (Ac) and the temperature difference between vapours (T_{vc}) and surface (T_{wc}) in the condenser region is known as condenser heat transfer coefficient (h_c) and the same is calculated using the Eq.(5).

$$h_c = \frac{Q_c}{A_c[T_{vc} - T_{wc}]} \tag{5}$$

The heat rejected at the condenser is calculated using the Eq. (6). T_{cwo} and T_{cwi} represent cooling water outlet and inlet temperatures.

$$Q_c = mc_p\left[T_{cwo} - T_{cwi}\right] \tag{6}$$

The ratio of length of heat pipe (L) to the product of thermal resistance of heat pipe (R_t) and cross sectional area of heat pipe is known as effective thermal conductivity of heat pipe (K_{eff})) and the same is calculated using the Eq. (7).

$$K_{eff} = \frac{L}{R_t.A} \tag{7}$$

2.3. Uncertainty analysis

An uncertainty analysis for the various parameters involved in experiments are calculated as follows. The uncertainty associated with applied heat load consists of uncertainties in voltage (V) and current (I). It is calculated using the Eq. (8).

$$\frac{\Delta Q}{Q} = \sqrt{\left(\frac{\Delta V}{V}\right)^2 + \left(\frac{\Delta I}{I}\right)^2} \tag{8}$$

The uncertainty in thermal resistance of the heat pipe consists of uncertainties in applied heat input (Q) and the temperature difference between evaporator and condenser and the same is calculated using the Eq. (9). Where (ΔT_{ec}) is the actual temperature difference between evaporator and condenser.

$$\frac{\Delta R_t}{R_t} = \sqrt{\left(\frac{\Delta Q}{Q}\right)^2 + \left(\frac{\Delta(\Delta T)}{\Delta T_{ec}}\right)^2} \tag{9}$$

The uncertainty in heat transfer coefficient at evaporator and condenser has uncertainties of heat flux (q) and corresponding temperature difference between surface and vapour (ΔT_{vs}) and the same is calculated using the Eq. (10).

$$\frac{\Delta h}{h} = \sqrt{\left(\frac{\Delta q}{q}\right)^2 + \left(\frac{\Delta(\Delta T)}{\Delta T_{vs}}\right)^2} \tag{10}$$

From the uncertainly analysis it is observed that the maximum uncertainly with heat input, heat pipe thermal resistance, and heat transfer coefficients are 1.2%, 2.47%, and 5.21% respectively.

3. Results and discussion

A set of experiments are done with water and PCM using acetone as the working fluid in a screen mesh heat pipe for different heat inputs (10W, 20W, 30W, 40W and 50W) and different flow rates of condenser coolant (10 LPH, 8.5 LPH, 7.5 LPH and 6 LPH). Fig. 2 shows the variation in the temperature of PCM and water with respect to time at different heat inputs at the heater.

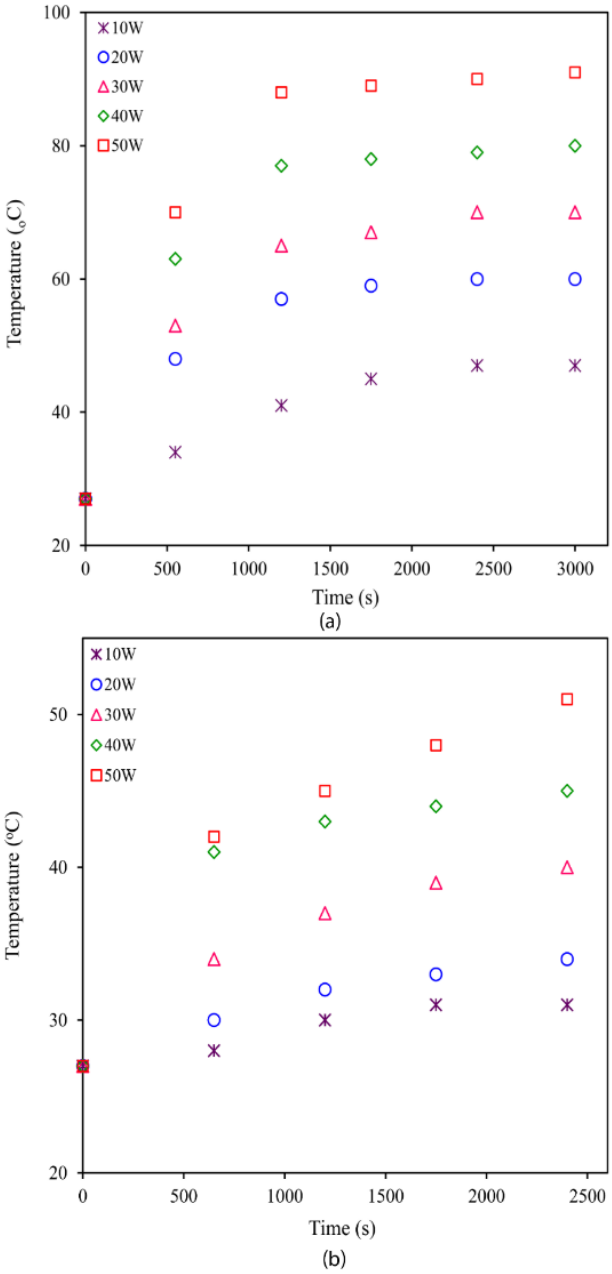

Fig.2 Variation of temperature with time during heating process at 10 LPH (a) PCM, (b) water

As heat load increases, the temperature of PCM/water also increases and the temperature reaches a steady state value after a few minutes. The time required to reach steady state is different for both PCM and water. This can be explained as follows: When heat is applied, the PCM layers adjacent to the heater absorbs heat by conduction. But, the heat transfer to the entire PCM material is delayed by low thermal conductivity and thermal storage capability of PCM. OM32 has a thermal conductivity of 0.219W/mK in solid state and 0.145W/mK in liquid state. Similarly, the melting point of OM32 is 33^{o}C. So when the temperature of PCM reaches the melting point, the PCM melts and it is converted into liquid. When PCM melts, natural convection heat transfer also occurs from the heater surface to the PCM. Convection can also dominate conduction when all the PCM is converted to liquid state.

The PCM temperature reached 90^{o}C whereas it is only 55^{o}C with water for a heat input of 50W with the same time interval. An increase of 63.6% in temperature is observed with the use of PCM

when compared with that of the water. The PCM tries to confine the heat for longer duration and this results in more heat retention time for PCM compared to water. The temperature of the PCM increases when it tries to retain the heat instead of giving it to heat pipe. The increase in temperature and longer duration to reach steady state is an indication of the better heat storage capacity of PCM.

Fig. 3 shows the variation in the temperature of PCM and water with respect to time at different heat inputs during cooling.

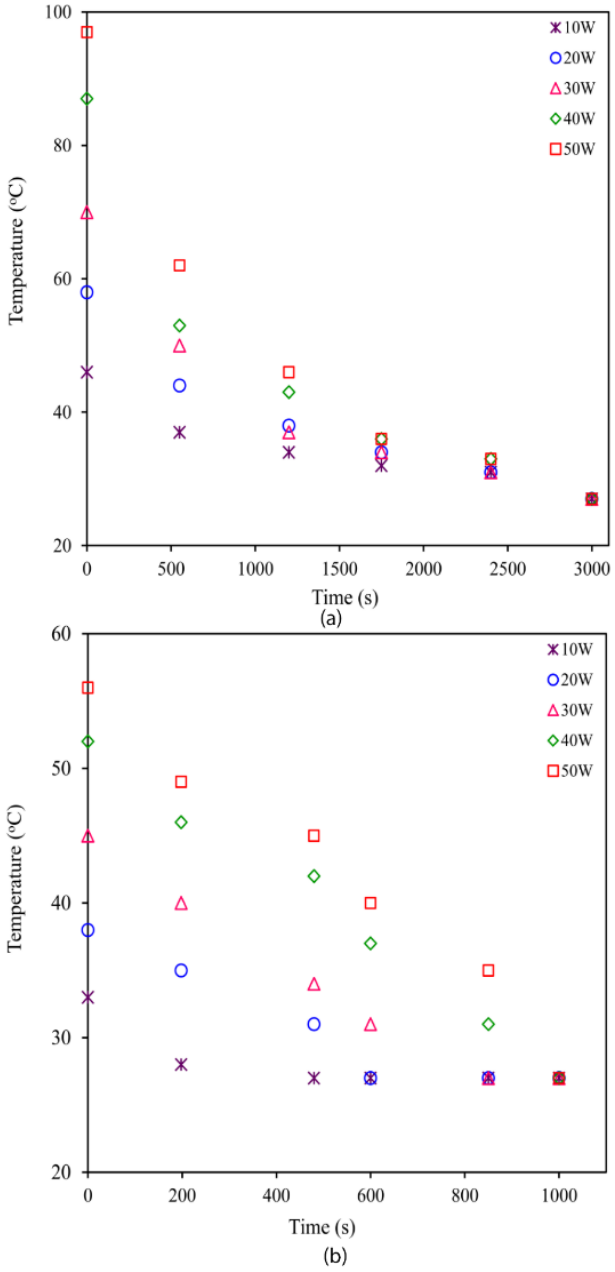

Fig. 3 Variation temperature with time during cooling process at 10 LPH (a) PCM, (b) water

It is observed from Fig. 3 that the PCM takes more time (3000s) for reaching the freezing point of 27°C from 90°C at 50 W heat load. However, the water reaches the freezing point of PCM within 1000 seconds at the same heat load. It shows that there is an enhancement of 200% in the heat retention time with the use of PCM when compared to that of water. This can be explained as follows:

During cooling, the heater is switched off and the heat pipe continues to transfer heat to condenser. The PCM/water layers adjacent to the evaporator of the heat pipe will be cooled easily. Since the thermal conductivity of PCM is low and thermal storage capability is high compared to water, the PCM layers located away from the heat pipe are not cooled easily. Since the freezing point of water is very low, convection and conduction heat transfers occur in water which helps in the fast cooling. In the case of PCM, convection is prevented when PCM starts to solidify. Hence, the heat retention capability of PCM is higher compared to water.

Fig. 4 shows the comparison of the time required to reach the steady state for heating and cooling of PCM and water for different heat inputs. It shows that as heat load increases the time required to reach steady state in heating process decreases for both PCM and water. It is due to lower thermal resistance at higher heat loads. Similarly, PCM melts easily and both conduction and convection contribute to the heat transfer. In the case of water, its thermal conductivity is high compared to PCM and convection heat transfer is the dominant mode of heat transfer. It can be seen that the cooling and heating of PCM takes longer time compared to water. For a heat load 50W and a flow rate of 10 LPH, the water reaches a steady state temperature of 55^0C within 1000s during heating and it takes 1000s to return back to the atmospheric condition, whereas the PCM takes 1500s to reach steady state for a temperature of 90^0C and 3000s to reach the same atmospheric condition. In both cases of PCM and water, the atmospheric condition is taken as 27^0C which is the freezing point of PCM.

Fig. 4 shows the comparison of the time required to reach the steady state for heating and cooling of PCM and water for different heat inputs.

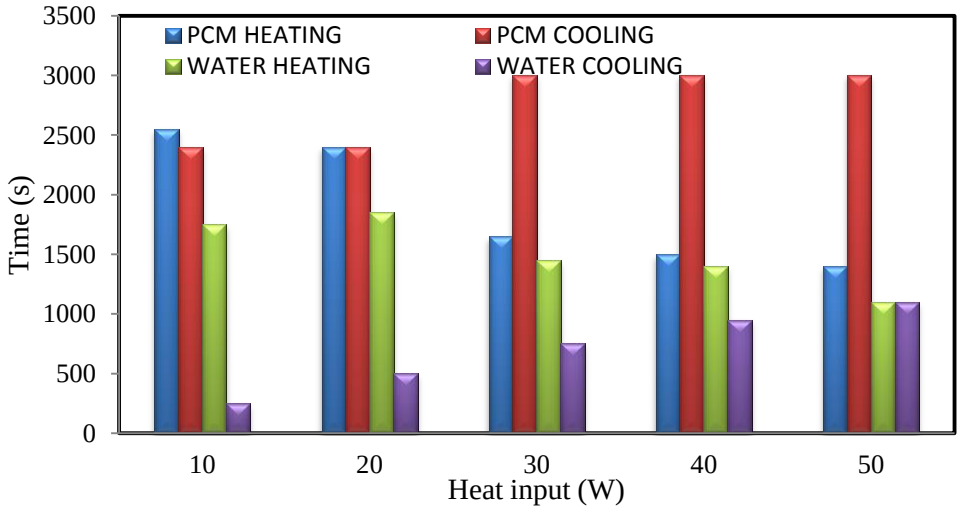

Fig. 4 Variation of time with respect heat input during heating and cooling of PCM and water

It shows that as heat load increases the time required to reach steady state in heating process decreases for both PCM and water. It is due to lower thermal resistance at higher heat loads. Similarly, PCM melts easily and both conduction and convection contribute to the heat transfer. In the case of water, its thermal conductivity is high compared to PCM and convection heat transfer is the dominant mode of heat transfer. It can be seen that the cooling and heating of PCM takes longer time compared to water. In both cases of PCM and water, the atmospheric condition is taken as 27^0C which is the freezing point of PCM.

The PCM holds more heat instead of giving it to the heat pipes. Hence, its steady state temperature is higher than water. In PCM, the heat storage takes place first as sensible heat and later as latent heat without affecting it properties [40]. When PCM reaches its melting point, the heat applied at evaporator is stored as latent heat and this heat is first released during the cooling process until the liquid PCM reaches the freezing point.

The variation of the average steady state wall temperature of evaporator (Te) and condenser (Tc) of the heat pipe with water and PCM at evaporator for different heat inputs and flow rates is shown in Fig. 5.

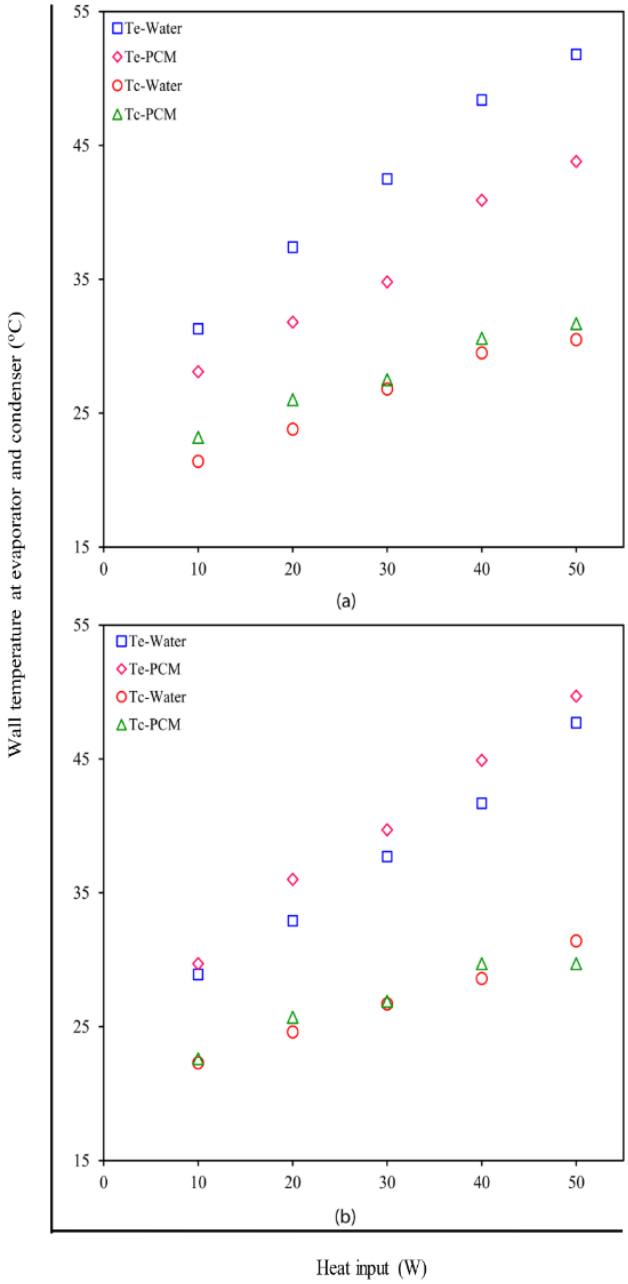

Fig. 5 Variation of wall temperature at evaporator and condenser with respect to heat input for (a) 10 LPH, (b) 7.5 LPH

The evaporator temperature increases with increase in heat load and with the use of PCM. This was due to more heat transfer at higher heat loads from the heater to the PCM/water. When heat is

reached at the evaporator of the heat pipe, the working fluid inside the heat pipe absorbs heat and it is vapourised. The vapours formed at the evaporator travel to condenser because there is a pressure difference between evaporator and condenser. At the condenser, vapours are get condensed into liquid and returns back to evaporator through the capillary wick, Since the heat pipe is in contact with water or PCM, the heat pipe shows higher evaporator temperature with PCM due to its high thermal storage capability. The low thermal conductivity of PCM also contribute to high evaporator temperature with its high conduction thermal resistance. In the case of PCM, the amount of heat reaching the evaporator is less compared to water. The condenser temperature variation is negligible for both water and PCM and it represents sufficient cooling of the working fluid at condenser at all heat loads. Similarly the effect of flow rate at condenser is found to be negligible for water and PCM. This is due to sufficient cooling that takes place at all flow rates.

Fig. 6 shows the variation of effective thermal conductivity of heat pipe with different heat inputs at the heater block. Effective thermal conductivity increases with increase in the heat input for both PCM & water and its value is higher for water for the same heat load applied at the heater [29, 30]. This can be explained as follow: At higher heat loads, more heat is transferred from the heater to the heat pipe through water or PCM. It results in lower thermal resistance and higher effective thermal conductivity values of the heat pipe. The effective thermal conductivity values of PCM is lower than that of water for all heat loads. It is due to the decrease in active heat load at evaporator of the heat pipe when PCM is used. Moreover, the low thermal conductivity and heat holding capability of PCM increases the thermal resistance of the heat flow from PCM to the heat pipe. At 10W, the effective thermal conductivity of heat pipe for PCM and water are 1674.5W/mK and 1800W/mK respectively and at 50 W, the corresponding values are 3376.2W/mK and 3748.9W/mK. These values represent an increase of 7.5% and 9.9% in K_{eff} for water. Initially, the heat is transferred from PCM to heat pipe by pure conduction. But when PCM melts, the heat transfer occurs by both conduction and convection leading to higher K_{eff} values at higher heat loads for PCM.

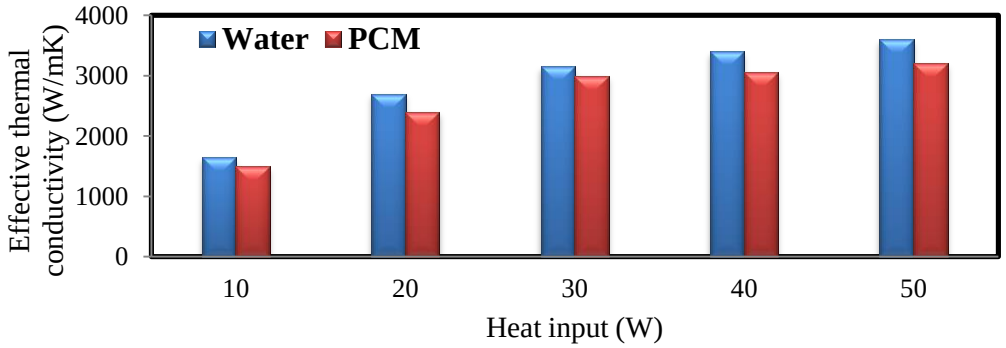

Fig.6 Variation of effective thermal conductivity of heat pipe with respect heat input

Fig. 7 shows the variation in the thermal resistance of the heat pipe with respect to applied heat load. It shows that the thermal resistance of the heat pipe decreases with increase in heat input and the thermal resistance of PCM is found to be higher than that of water for all the heat loads. This can be explained as follows: When heat load increases, more heat is transferred from the heater to the working fluid of the heat pipe through PCM or water. This leads to more vapourization heat transfer from evaporator to condenser. Hence, lower values of thermal resistances are obtained at higher heat loads [41]. Since PCM has high thermal storage capacity and low thermal conductivity compared to water, the amount of heat reaching the evaporator of heat pipe is less. This results decrease in

vapourization and higher thermal resistance values compared to water. At 10W, thermal resistance of water and PCM are 0.767 K/W and 0.825 K/W respectively and for 50 W, the corresponding values are 0.368K/W and 0.409K/W. It indicates that the thermal resistance of PCM is 7.03% and 10.02% higher than water at 10W and 50W respectively.

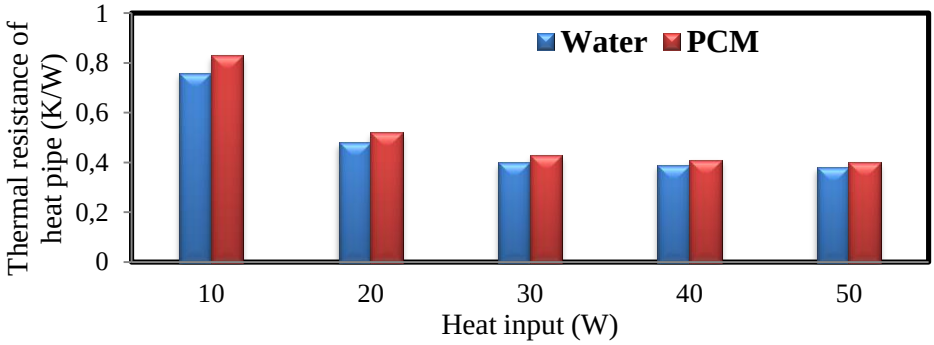

Fig. 7 Variation of thermal resistance of heat pipe with respect heat input

The evaporator heat transfer coefficient as a function of heat input is shown in Fig. 8. The factors affecting evaporator heat transfer coefficient are evaporator surface and vapour temperatures, evaporator surface area, latent heat of vaporization, heat load and fill ratio. Evaporator heat transfer coefficient increases with increase in heat load and it is due to the enhancement in rate of boiling at evaporator of heat pipe. The decrease in temperature difference between the evaporator surface and vapour gives rise higher h_e values at high heat loads. The h_e values of heat pipe are higher for water compared to PCM for all the heat inputs and it is due to high active heat loads at the evaporator. At 10W and 50W, an increment of 65.4% and 50.5 % are observed in h_e with water compared to PCM.

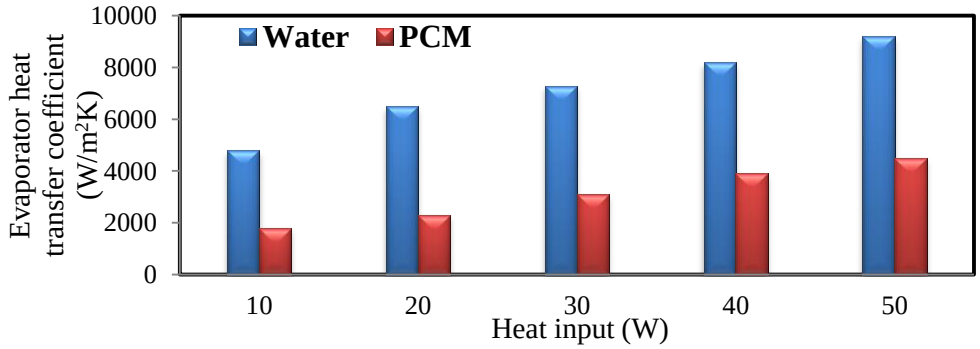

Fig.8 Variation of evaporator heat transfer coefficient of heat pipe with respect heat input

The condenser heat transfer coefficient (h_c) as a function of heat input is shown in Fig. 9. The h_c values are mainly influenced by vapour temperature, area and surface properties of condenser, cooling water flow rate and its temperature. Condensation heat transfer coefficient decreases with increase in heat load and it is higher for water. It is due to the increase in temperature difference between vapour and wall at condenser [15]. Moreover, at higher heat loads more vapours reach condenser leading to higher vapour temperature at condenser. Since the area of condenser is same for all heat inputs, the condensation heat transfer coefficient decreases. The evaporation rate is higher for water compared to PCM at all heat loads. This causes more vapours to reach the condenser for more condensation heat transfer. Hence higher values of h_c are obtained for water compared to PCM. At 10W and 50W, the

condensation heat transfer coefficient shows an increase of 20.26% and 20.76 % respectively with water compared to PCM and it is due the difference in boiling rate at evaporator.

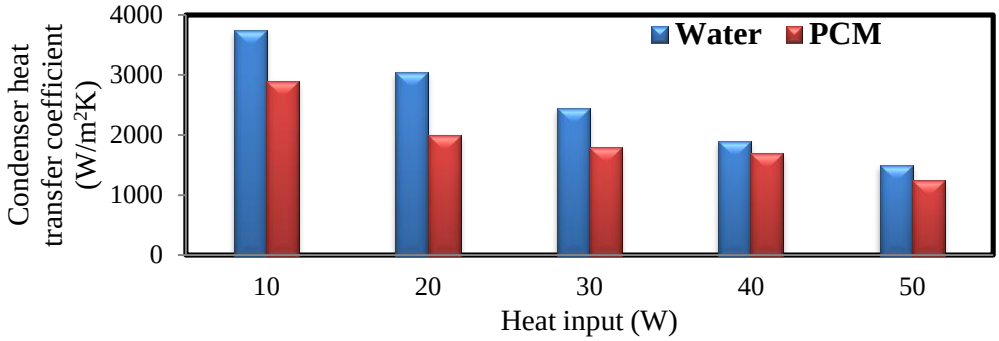

Fig. 9 Variation of condenser heat transfer coefficient of heat pipe with respect heat input

Conclusion

An experimental study was conducted to analyse the thermal performance of a PCM-heat pipe system using OM32 and acetone as PCM and heat working fluid respectively in a heat load range of 10-50W for different flow rates of condenser coolant. The heat was supplied to the evaporator of the heat pipe through a container filled with PCM or water. In this study, the heating and cooling of PCM and water were analysed at various heat loads. The experimental results showed that the PCM reached higher steady state temperatures and took more time for heating and cooling cycles compared to water. For the highest heat load of 50W, the steady state temperature of PCM was 63.6% higher than water during heating and time required to reach the atmospheric temperature during cooling was 200% more than that of water. Similarly the thermal resistance and evaporator temperature were higher and heat transfer coefficients were lower for PCM compared to water at all heat loads. For 50W, the thermal resistance was 10.02% higher, evaporator heat transfer coefficient, condenser heat transfer coefficient and effective thermal conductivity were 50.5 %, 20.76%and 9.9% respectively lower for PCM compared to water. It was due the change in active heat load applied at the evaporator of the heat pipe. These results indicates that PCM has higher heat retention capability to use it for thermal storage applications. Similarly, water is better than OM32 if this PCM-heat pipe is used for electronics cooling applications.

Acknowledgment

The authors would like to thank Mr. R Jaya Seelan, of Karunya University for helping in the fabrication of the experimental test facility. The third author gratefully appreciate the financial assistance provided by the funding agency, the Department of Science and Technology (DST), Science and Engineering Research Board (SERB), (SB/FTP/ETA-362/2012), New Delhi, India. The fifth author acknowledges the support provided by the "Research Chair Grant" National Science and Technology Development Agency (NSTDA), the Thailand Research Fund (TRF) and King Mongkut's University of Technology Thonburi through the "KMUTT 55th Anniversary Commemorative Fund".

Nomenclature

LPH	litres per hour	Subscripts	
V	voltage (V)	e	evaporator
I	current (A)	c	condenser
c_p	specific heat of cooling water (J/kg K)	ve	vapour at evaporator
A_e	area of the evaporator (m^2)	vc	vapour at condenser
A_c	area of the condenser (m^2)	we	wall at evaporator
Q_e	heat input at the storage tank (W)	wc	wall at condenser

References

[1] Chen, B.R., et al., Long-term thermal performance of a two-phase thermo syphon solar water heater, Solar Energy 83 (2009) pp. 1048–55.

[2] Fok, S. C., et al., Cooling of portable hand-held electronic using phase change materials in finned heat sinks, International Journal of Thermal Sciences 49 (2010) pp. 109–17.

[3] Lu, T. J., et al., Thermal management of high power electronics with phase change cooling. International Journal of Heat and Mass Transfer 43 (2000) pp. 2245–2256.

[4] Pasupathy, A., et al., Phase change material-based building architecture for thermal management in residential and commercial establishments, Renewable and Sustainable Energy Reviews 12 (2008) pp. 39–64.

[5] Chen, S.L., et al., An experimental investigation of cold storage in an encapsulated thermal storage tank, Experimental Thermal and Fluid Sciences 23 (2000) pp. 133–44.

[6] Arshad, A., et al., An experimental study of enhanced heat sinks for thermal management using n-eicosane as phase change material, Applied Thermal Engineering 132 (2018) pp. 52–66.

[7] Ali, H. M. and Arshad, A., Experimental investigation of n-eicosane based circular pin-fin heat sinks for passive cooling of electronic devices, International Journal of Heat and Mass Transfer 112 (2017) pp. 649–661.

[8] Arshad, A., et al., Experimental investigation of PCM based round pin-fin heat sinks for thermal management of electronics: Effect of pin-fin diameter, International Journal of Heat and Mass Transfer 117 (2018) pp. 861–872.

[9] Ashraf, M. J., et al., Experimental passive electronics cooling: Parametric investigation of pin-fin geometries and efficient phase change materials, International Journal of Heat and Mass Transfer 115 (2017) pp. 251–263.

[10] Yoo, D. W., et al., Energy efficient thermal management of electronic component using solid–liquid phase change material, IEEE Transactions on Device and Materials Reliability 4 (2004) pp. 641–649.

[11] Zheng, N., et al., A hybrid thermal energy storage device, part 1: design methodology, Journal of Electronic Packaging 126 (2004) pp. 1–7.

[12] Zheng, N., et al., A hybrid thermal energy storage device, part 2: thermal performance figures of merit, Journal of Electronic Packaging 126 (2004) pp. 8–13.

[13] Wang, X. Q., et al., Effect of orientation for phase change material (PCM)-based heat sinks for transient thermal management of electric components, International Communications in Heat and Mass Transfer 34 (2007) pp. 801–808.

[14] Yin, H., et al., Experimental research on heat transfer mechanism of heat sink with composite phase change materials, Energy Conversion and Management 49 (2008) pp. 1740–1746.

[15] Asirvatham, L. G., et al., Heat transfer performance of screen mesh wick heat pipes using silver-water nanofluid, International Journal of Heat and Mass Transfer 60 (2013) pp. 201-209.

[16] Kumaresan, G., et al., Comparative study on heat transfer characteristics of sintered and mesh wick heat pipes using CuO nanofluids, International Communications in Heat and Mass Transfer 57 (2014) pp. 208-215.

[17] Godson, L., et al., Enhancement of heat transfer using nanofluids-An overview, Renewable and Sustainable Energy Reviews 14 (2) (2010) pp. 629-641.

[18] Asirvatham, L. G., et al., Operational limitations of heat pipes with silver-water nanofluids, Journal of Heat Transfer, 135 (2013) pp. 111011 1-10.

[19] Tharayil, T., et al., Effect of nanoparticle coating on the performance of a miniature loop heat pipe for electronics cooling applications, Journal of Heat Transfer, 140 (2) (2017) pp. 022401-09.

[20] Ninolin, E., et al., Thermal Performance of a Compact Loop Heat Pipe with Silver-Water Nanofluid, Applied Mechanics and Materials 852 (2016) pp. 666-674.

[21] Asirvatham, L. G., et al., Convective heat transfer of nanofluids with correlations, Particuology 9 (2011) pp. 626-631.

[22] Solomon, A. B., et al., Heat transfer performance of an anodized two-phase closed thermosyphon with refrigerant as working fluid, International Journal of Heat and Mass Transfer 82 (2015) pp. 521–529.

[23] Tharayil, T., et al., Performance of cylindrical and flattened heat pipes at various inclinations including repeatability in anti-gravity – A comparative study, Applied Thermal Engineering 122 (2017) pp. 685–696.

[24] Tharayil, T., et al., Entropy generation analysis of a miniature loop heat pipe with graphene-water nanofluid: Thermodynamics model and experimental study, International Journal of Heat and Mass Transfer (2017) pp. 407-421.

[25] Asirvatham, L. G., et al., Heat transfer performance of a glass thermosyphon using graphene-acetone nanofluid, Journal of Heat Transfer 137 (2015) pp. 111502 1-9.

[26] Kumaresan, G., et al., Experimental investigation on enhancement in thermal characteristics of sintered wick heat pipe using CuO nanofluids, International Journal of Heat and Mass Transfer 72 (2014) pp. 507-516.

[27] Ramachandran, R., et al., Comparative study of the effect of hybrid nanoparticle on the thermal performance of cylindrical screen mesh heat pipe, International Communications in Heat and Mass Transfer 76 (2016) pp. 294–300.

[28] Solomon, A. B., et al., Numerical analysis of a screen mesh wick heat pipe with Cu/water nanofluid, International Journal of Heat and Mass Transfer 75 (2014) pp. 523–533.

[29] Tharayil, T., et al., Effect of filling ratio on the performance of a novel miniature loop heat pipe having different diameter transport lines, Applied Thermal Engineering 106 (2016) pp. 588-600.

[30] Tharayil, T., et al., Thermal performance of miniature loop heat pipe with graphene-water nanofluid, International Journal of Heat and Mass Transfer 93 (2016) pp. 957-968.

[31] Ladekar, C. L., et al., Experimental Investigate for Optimization of Heat Pipe Performance in Latent Heat Thermal Energy Storage, Materials Today: Proceedings 4 (2017) pp. 8149–8157

[32] Wu, W. et al., Experimental investigation on the thermal performance of heat pipe-assisted phase change material based battery thermal management system, Energy Conversion and Management 138 (2017) pp. 486–492.

[33] Tiari, S., et al., Experimental study of a latent heat thermal energy storage system assisted by a heat pipe network, Energy Conversion and Management 153 (2017) pp. 362–373.

[34] Motahar, S. and Khodabandeh, R., Experimental study on the melting and solidification of a phase change material enhanced by heat pipe, International Communications in Heat and Mass Transfer, 73 (2016) pp. 1-6.

[35] Gui, X., et al., Influence of void ratio on phase change of thermal energy storage for heat pipe receiver, Thermal Science 19 (3) (2015) pp. 967-976

[36] Tso, C. P., et al., Transient and cyclic effects on a PCM-cooled mobile device, Thermal Science 19 (5) (2015) pp. 1723-1731.

[37] Nasehi, R., et al., Using multi-shell phase change materials layers for cooling a lithium-ion battery, Thermal Science 20 (2) (2016) pp. 391-403.

[38] Al-Hamadani, A. A. and Shukla, S. K., Modelling of solar distillation system with phase change material storage medium, Thermal Science 18 (2) (2014) pp. S347-S362.

[39] Arasu, A. V., et al., Numerical performance study of paraffin wax dispersed with alumina in a concentric pipe latent heat storage system, Thermal Science 17 (2) (2013) pp. 419-430

[40] Weng, Y. C., et al., Heat pipe with PCM for electronic cooling, Applied Energy 88 (2011) pp. 1825-1833.

[41] Tharayil, T., et al., Thermal Management of Electronic Devices Using Combined Effects of Nanoparticle Coating and Graphene–Water Nanofluid in a Miniature Loop Heat Pipe, IEEE Transactions On Components, Packaging and Manufacturing Technology, 8 (7) 2018 pp. 1241-1253.